J. Fluid Mech. (1988), *vol.* 193, *pp.* 53–74
Printed in Great Britain

Sound waves in monodisperse gas–particle or vapour–droplet mixtures

By N. A. GUMEROV[†], A. I. IVANDAEV[‡] AND R. I. NIGMATULIN[‡]

[†] Department of Mechanics and Mathematics of M. V. Lomonosov Moscow University, Moscow, 117234, USSR

[‡] Institute of North Problem Development of the USSR Academy Siberian Branch, Tumen, Post Box 2774, 625003, USSR

(Received 5 August 1986 and in revised form 27 October 1987)

A brief review of the relevant papers and an examination of the current status of research in the field of the acoustics of gas–particle suspensions are given. Non-stationary momentum, mass and energy transfer processes between a gas (vapour) and dispersed particles (droplets) under high-frequency acoustic perturbations are considered. A comparative evaluation of characteristic times and temperature differences for gas–particle and vapour–droplet mixtures subjected to acoustic perturbation is given. General dispersion equations to describe the propagation of weak monochromatic waves for a wide range of frequencies complying with the requirements of the acoustic homogeneity of the medium are derived. Frequency dependences of propagation velocity and attenuation coefficient of weak waves in water vapour–droplet mixtures are investigated. Frequency ranges are indicated over which different types of approximate theories are valid.

1. Introduction

The effect of suspended particles on the propagation of sound in a gas was discussed by Sewell (1910) who was probably the first to investigate the attenuation of audible sound in fogs. Sewell derived a formula for calculating the absorption of sound at different frequencies due to interfacial drag forces and scattering of waves by droplets. He assumed droplets to be immovable rigid particles and neglected the heat and mass transfer between them and a gas.

Sewell's formula ignores a number of real effects and dissipative mechanisms. One of its imperfections was already clear to Lamb (1945) who pointed out that the absorption coefficient of Sewell tends to zero under reducing droplet size (the corollary of assuming droplets to be frozen in the wave). Having allowed for the motion of particles, Lamb obtained a more general formula for the coefficient of attenuation.

Rytov, Vladimirsky & Galanin (1938) analysed the propagation of perturbations in barotropic systems, taking into account only the non-stationary effects of interfacial force interaction. Similar results were obtained in the same period by Viglin (1938) and Oswatititsch (1941), who studied the effect of non-equilibrium phase transitions on the propagation of sound in one-component two-phase vapour–droplets mixture (wet steam). However, Viglin and Oswatititsch used the very strong simplifying assumptions of equal velocities and temperatures of the phases in the wave. The effect of non-stationary heat transfer between phases on the attenuation of acoustic waves in two-phase mixtures seems to have been discussed first by Isakovich (1948).

A more detailed survey of the above-mentioned work, and some other papers published prior to 1960, can be found in the monographs of Bergmann (1954) and Richardson (1962). Some aspects of the state of the field have been discussed in various reviews and monographs (Landau & Lifshitz 1954; Fuks 1955; Soo 1967; Deich & Filippov 1968; Isakovich 1973).

The propagation of small perturbations has been given the most attention. Epstein & Carhart (1953), Kleiman (1958, 1961), Zink & Delsasso (1958), Soo (1960), Chow (1964), Temkin & Dobbins (1966*a*), Popov (1968, 1970), Mori, Hijikata & Kamada (1971) studied the speed and attenuation of sound in a gas carrying small particles of a solid inert phase, in the absence of phase transformations. These authors took into account the effects of heat transfer between phases; however they ignored the non-stationary effects of interfacial interactions. An attempt to cover these effects for the ultrasonic range of frequencies was made by Popov (1970). Soo (1960) discussed peculiarities in propagation through smoke-type polydisperse aerosols with low mass concentration of the condensed phase.

A number of papers have treated the dispersion and absorption of weak perturbations in vapour– and gas–droplet mixtures under phase transformations (Städtke 1968; Ivandaev & Nigmatulin 1970; Ivandaev 1978; Gumerov, Ivandaev & Nigmatulin 1983).

Dispersion and attenuation of low-frequency acoustic perturbations in vapour and vapour–gas fogs at low mass concentrations m of the condensed phase ($m \ll 1$) were studied by Cole & Dobbins (1970), Marble (1970), Marble & Wooten (1970), Davidsion (1975*b*), Rosenfeld (1983). It was shown that in this case a maximum of attenuation per wavelength is observed at dimensionless frequencies $\omega\tau_v \sim m$, i.e. at $\omega\tau_v \ll 1$ (where ω is the circular frequency and τ_v is the Stokes relaxation time between gas and particle velocities).

In a number of papers the propagation of weak perturbations in heterogeneous media has been studied, taking into account some additional factors such as the initial non-uniformity of the medium, radiation and some other physico-chemical factors (Stasenko 1973; Lymon & Chen 1978; Meyer zur Cappelen 1981). Attenuation of the acoustic wave in a non-uniform medium with temperature and density gradients in the direction of the wave propagation can be greatly different from that in the corresponding uniform system (Lymon & Chen 1978).

The attenuation of weak discontinuities in gas–particle mixtures for planar, cylindrical and spherical symmetries of flow has been studied by Bhutani & Chandran (1977).

In a series of recently published papers the propagation of weak shock waves in gas–particle mixtures has been studied (Rochelle & Peddieson 1976; Rasmussen 1977; Nikaien, Peddieson & Au 1983).

Much attention has been paid to the study of weak nonlinear perturbations in a gas with particles. The starting system of differential equations in some simplified variant can be reduced to only one Burgers-type equation. Quite a few papers aim at deriving such an equation since its main properties are relatively well known (Davidson & Scott 1973; Davidson 1975*a*, 1976; Borisov, Vakhgelt & Nakoryakov 1980, 1981; Tarakanov & Todes 1982). Some authors have studied the propagation of finite-amplitude rarefaction and compression waves in gas–particle mixtures by the method of characteristics (Yamamoto, Kobayashi & Takano 1980).

The above-mentioned papers treat the propagation of perturbations in sufficiently dilute gas–particle mixtures for the effects of direct interaction between particles of the dispersed phase to be negligible. Among the others dealing with wave propagation in concentrated suspensions we can single out the recently published articles of Buevich & Fedotov (1980) and Ryzhkov & Tolmachev (1983).

The work of Altberg & Holzman (1925), who measured the attenuation of acoustic vibrations with frequencies from 0.5 to 2 kHz in smoke-type aerosols, appears to be among the earliest experimental studies of sound in gas–particle mixtures. The qualitative data on sound attenuation reported by Knudsen (1931), were probably the first for humid air.

Experimental data on the absorption of sound at 42, 98 and 659 kHz in smokes of stearic acid and magnesium oxide, as well as in an aerosuspension of monodisperse lycopodium powder of 5 μm particle size, were obtained by Laidler & Richardson (1938). Knudsen, Willson & Anderson (1948) reported data on the attenuation of low-frequency sound at 500 Hz in a polydisperse fog generated by atomizing water in the air. In all these experiments only the absorption of acoustic waves was measured; the speed of sound was not studied.

The first measurements of the attenuation and dispersion of acoustic vibrations in gas–particle mixtures were carried out by Zink & Delsasso (1958). They worked with polydisperse suspensions of spherical Al_2O_3 particles in gases with different thermal properties: hydrogen, oxygen, helium and argon. Particle diameter was from 5 to 15 μm, and frequency was varied from 0.5 to 13.6 kHz. The corresponding values of dimensionless frequency $\omega\tau_v$ in these experiments exceeded unity.

Data on dispersion and attenuation of sound in a mixture of oleic acid droplets and a nitrogen carrier gas at dimensionless frequency $\omega\tau_v \sim 1$ can be found in Dobbins & Temkin (1964) and Temkin & Dobbins (1966*b*). The experiments were carried out for mass concentrations of droplets from 10^{-2} to 2×10^{-2}, and the frequency was varied from 1 to 9.5 kHz. The mean droplet diameter varied in different experiments from 0.8 to 4.7 μm. The mass concentration and droplet diameters were measured optically. It was shown that the maximum of sound attenuation per wavelength is achieved when $\omega\tau_v \sim 1$.

Cole & Dobbins (1971) reported some interesting results on the speed and attenuation of sound in air fog. The fog was generated in a Wilson cloud chamber. Experiments were carried out for the range of droplet diameters from 2 to 10 μm at 80 Hz and mass concentration of the liquid phase $m \sim 10^{-2}$. The maximum of attenuation per wavelength was observed not at $\omega\tau_v \sim 1$, as in the case of a gas–particle mixture, but at $\omega\tau_v \sim m$.

Most experiments have been conducted with sound propagation through polydisperse suspensions, with practically no information on the particle size distribution functions. Even in the most careful experimental studies (Cole & Dobbins 1971; Temkin & Dobbins 1966*b*) only two parameters were measured directly: a certain 'volume-to-surface' mean diameter of particles and their mass concentration in the mixture. That is why it is quite difficult to compare a theory with the experiments.

No systematic experimental data have been reported in the literature on the speed and attenuation of sound in systems with different thermal properties of the phases. Very limited data are available to analyse the effect of phase transformations on the shape of dispersion curves. Nothing is known of attenuation at high frequencies, when the non-stationary effects of interaction between phases are significant. It would be of considerable theoretical and practical interest if data of this kind were obtained for mono- and polydisperse systems with a known particle size distribution function.

2. General linearized equations and the laws of interaction between phases in high-frequency acoustic fields

If finely dispersed particles or droplets of a solid or liquid substance are uniformly distributed in a carrying gas or vapour, and the wavelength of sound is much greater than the size of the particles and interparticle distances, the vapour– or gas–particle mixture is an acoustically homogeneous continuum. Propagation of small perturbations in such a medium can be described by linearized conservation equations of masses, momenta and energies of the phases. They follow from the general nonlinear equations of motion for two-phase mixtures of dispersed structure (see Nigmatulin 1978, 1979).

2.1. *Linearized equations of motion and state*

Linearized conservation equations of mass, momentum and energy for the planar one-dimensional motion of a dilute mixture in a reference frame where an initially equilibrium heterogeneous mixture is at rest ($u_{10} = u_{20} = u_0 = 0$) can be written in the form (see Ivandaev 1978)

$$\left.\begin{aligned} \frac{\partial \rho_1}{\partial t} + \rho_{10}\frac{\partial u_1}{\partial x} = -n_0 j, \quad \frac{\partial \rho_2}{\partial t} + \rho_{20}\frac{\partial u_2}{\partial x} = n_0 j, \\ \rho_{10}\frac{\partial u_1}{\partial t} + \frac{\partial p}{\partial x} = -n_0 f, \quad \rho_{20}\frac{\partial u_2}{\partial t} = n_0 f; \end{aligned}\right\} \tag{1}$$

$$\rho_{10}\frac{\partial i_1}{\partial t} = \alpha_{10}\frac{\partial p}{\partial t} - n_0 q_{1\sigma}, \quad \rho_{20}\frac{\partial e_2}{\partial t} = -n_0 q_{2\sigma}, \quad q_{1\sigma} + q_{2\sigma} = -jl_0, \tag{2}$$

$$\rho_{10} = \alpha_{10}\rho_{10}^0, \quad \rho_{20} = \alpha_{20}\rho_{20}^0, \quad \alpha_{10} + \alpha_{20} = 1, \quad \alpha_{20} = \tfrac{4}{3}\pi a_0^3 n_0.$$

Here (1) are the mass and momentum conservation equations of the continuous (subscript 1) and the dispersed (subscript 2) phases, and (2) are the equations of heat influx to gas (vapour), particles (droplets) and the surface of an individual droplet. The symbols ρ, ρ^0, α, u, e and i denote, respectively, mean and true densities, volume fraction, velocity, internal energy and enthalpy; p is a pressure, a and n are the radius of particles and their number density, l is the latent heat of evaporation. The letters f, j and $q_{j\sigma}$ denote, respectively, the force applied by the gas to a droplet; the rate of condensation at the surface of an individual droplet; and the heat flux from the jth phase ($j = 1, 2$) to the surface of a droplet (subscript σ). Subscript 0 refers to the initial undisturbed state. Here we limit the analysis to a study of the initially uniform state of the mixture along the x-coordinate, i.e. ρ_{10}, ρ_{20}, n_0, α_{20}, a_0, p_0 are each constant.

The equations of state of a calorically perfect gas and an incompressible dispersed phase take, after linearization, the forms

$$\left.\begin{aligned} \frac{\mathrm{d}p}{p_0} = \frac{\mathrm{d}\rho_1^0}{\rho_{10}^0} + \frac{\mathrm{d}T_1}{T_0}, \quad \mathrm{d}i_1 = c_i\,\mathrm{d}T_1 \quad (c_1 = \text{const}), \\ \mathrm{d}\rho_2^0 = 0, \quad \mathrm{d}e_2 = c_2\,\mathrm{d}T_2 \quad (c_2 = \text{const}), \end{aligned}\right\} \tag{3}$$

where T is the temperature, and c_1 and c_2 are the specific heats of the gaseous (at constant pressure) and condensed phases.

To avoid confusion we shall drop the subscript 0 everywhere below.

Let us study the solutions of the system of linear equations (1)–(3), which have the form of travelling waves for perturbations $\mathrm{d}\chi = \mathrm{d}\rho_j, \mathrm{d}u_j, \mathrm{d}p, \ldots$:

$$\left.\begin{aligned} &\mathrm{d}\chi \sim \exp\{\mathrm{i}(k_* x-\omega t)\} = \exp(-k_{**}x)\exp\{\mathrm{i}(kx-\omega t)\} \\ &k_* = k+\mathrm{i}k_{**}, \quad C_\mathrm{p} = \frac{\omega}{k}, \quad C_\mathrm{g} = \frac{\mathrm{d}\omega}{\mathrm{d}k}, \quad \sigma = \frac{2\pi C_\mathrm{p} k_{**}}{\omega} \end{aligned}\right\} \tag{4}$$

where $\mathrm{i}^2 = -1$, k_* is the complex wavenumber, k_{**} is the linear attenuation coefficient; C_p, C_g and σ denote the phase velocity, group velocity and absorption coefficient per wavelength.

Note that although (1) and (2) are formally justifiable only when the wavelength $L_\omega = 2\pi C_\mathrm{p}/\omega$ is much greater than the characteristic distance between the particles $d = a\alpha_2^{-\frac{1}{3}}$ (i.e. at frequencies $\omega \ll \omega_\alpha$, where $\omega_\alpha = 2\pi C_\mathrm{p}/d$), in practice the equations are valid at frequencies $\omega \ll \omega_C$, where $\omega_C = \pi C_\mathrm{p}/a$. For waves with $L_\omega \gg a$ a gas–particle mixture may be considered as an acoustically homogeneous medium.

2.2. *Non-stationary effects in interfacial momentum transfer*

The total force acting on a spherical particle due to unsteady gas motion around it can be written as a sum of the four forces (see, for example, Nigmatulin 1978)

$$f = f_\mu + f_A + f_m + f_\mathrm{B}. \tag{5}$$

Here f_μ is the quasi-stationary viscous drag force (the Stokes force at low Reynolds numbers Re_{12} of the relative motion), f_A the buoyancy force, f_m the virtual mass force and f_B the Basset force due to the non-stationarity of the viscous boundary layer about the particle. In the case of weak perturbations, the formulae for these forces are

$$\left.\begin{aligned} &f_\mu = 6\pi a\mu_1(u_1-u_2), \quad f_A = \tfrac{4}{3}\pi a^3\rho_1^0 \frac{\partial u_1}{\partial t}, \quad f_m = \tfrac{2}{3}\pi a^3 \rho_1^0 \frac{\partial}{\partial t}(u_1-u_2), \\ &f_\mathrm{B} = 6a^2(\pi\rho_1^0\mu_1)^{\frac{1}{2}} \int_{-\infty}^{t} \frac{\partial}{\partial \tau}(u_1-u_2)\frac{\mathrm{d}\tau}{(t-\tau)^{\frac{1}{2}}}. \end{aligned}\right\} \tag{6}$$

Note that the momentum conservation equations of the phases (see (1)) can be written in the equivalent form

$$\rho_{10}\frac{\partial u_1}{\partial t} = -\alpha_{10}\frac{\partial p}{\partial x} - \alpha_{10}\, n_{10}(f_\mu + f_\mathrm{B} + f_m),$$

$$\rho_{20}\frac{\partial u_2}{\partial t} = -\alpha_{20}\frac{\partial p}{\partial x} + \alpha_{10}\, n_0(f_\mu + f_\mathrm{B} + f_m) \equiv n_0(f_A + f_\mu + f_\mathrm{B} + f_m).$$

Sometimes the term

$$-\alpha_{20}\frac{\partial p}{\partial x} \equiv n_o f_A + \alpha_{20}\, n_0(f_\mu + f_\mathrm{B} + f_m)$$

is called the ‘buoyancy’ force.

The solution of a wave dynamics problem for gas–particle mixtures becomes substantially more complicated if the Basset force is used to describe the motion history effect on the behaviour of dispersed particles. Difficulties are alleviated at high Re_{12} (e.g. in shock waves) because in this case the non-stationary effects of the interfacial force and thermal interaction (and especially Basset-type memory effects) are negligible.

At low Re_{12}, non-stationary effects often cannot be ignored. A typical case in which they must be taken into account is the weak monochromatic perturbation propagation problem. In this case the unknown functions are complex exponentials of coordinates and time (4), and the Basset force integral can be calculated as

$$f_{\mathrm{B}} = 3\sqrt{2}\,\pi a^2(1-\mathrm{i})(\rho_1^0\mu_1\omega)^{\frac{1}{2}}(u_1-u_2). \tag{7}$$

For the forces f_A and f_m we have, respectively,

$$f_A = -\mathrm{i}\omega\tfrac{4}{3}\pi a^3\rho_1^0 u_1, \quad f_m = -\mathrm{i}\omega\tfrac{2}{3}\pi a^3\rho_1^0(u_1-u_2). \tag{8}$$

We note that the forces f_A and f_m are of the same order of magnitude.

The f_m to f_μ, f_{B} to f_μ, and f_m to f_{B} ratios are frequency-dependent, the relevant oscillations being displaced in phase:

$$\left.\begin{gathered}\frac{f_m}{f_\mu} = -\frac{1}{9}\mathrm{i}(\omega\tau_{\mu1}); \quad \frac{f_{\mathrm{B}}}{f_\mu} = \frac{1-\mathrm{i}}{\sqrt{2}}(\omega\tau_{\mu1})^{\frac{1}{2}}; \quad \frac{f_m}{f_{\mathrm{B}}} = \frac{1-\mathrm{i}}{9\sqrt{2}}(\omega\tau_{\mu1})^{\frac{1}{2}}; \\ \tau_{\mu1} = \frac{a^2\rho_1^0}{\mu_1}; \quad \delta_{\mu1} = \left(\frac{\mu_1}{\rho_1^0\omega}\right)^{\frac{1}{2}}.\end{gathered}\right\} \tag{9}$$

Here $\delta_{\mu1}$ is the typical 'thickness' of the viscous boundary layer about a droplet (the 'penetration depth' of velocity perturbation into the gas over the characteristic time of oscillations $\tau = \omega^{-1}$), and $\tau_{\mu1}$ denotes the characteristic time over which a quasi-stationary, or Stokes, velocity field builds up in the gas around a particle.

The total force of interfacial interaction f is actually the Stokes viscous drag force only at sufficiently low frequencies, $\omega < 10^{-2}\tau_{\mu1}^{-1}$. At these frequencies it is independent of frequency, because velocity perturbations penetrate (due to viscosity) into the gas over the characteristic time of oscillations to a distance much greater than the droplet size ($\delta_{\mu1} \gg a$). At the same time the droplet size is much greater than the mean free path of molecules L in the continuous phase,

$$a \gg L \sim \mu_1/(\rho_1^0 C_1),$$

where C_1 is the speed of sound in the gaseous phase (for saturated steam at $p = 1.0$ MPa we have $C_1 \sim 500$ m/s and $L \sim 10^{-8}$ m). So,

$$\tau_{\mu1}^{-1} = \frac{\mu_1}{\rho_1^0 a^2} \sim \frac{L}{a}\frac{C_1}{a} \ll \omega_C \quad \left(\omega_C = \frac{\pi C_1}{a}\right)$$

where ω_C is the frequency limit.

There is, therefore, a wide range of high frequencies,

$$10^{-2}\tau_{\mu1}^{-1} \ll \omega \ll \omega_C,$$

in which forces f_{B}, f_m and f_A due to the non-stationarity of the gas flow around droplets, are comparable with the quasi-steady drag force f_μ, or even substantially exceed it. However, the gas–particle mixture can still be treated as a continuum, and the wave processes in it may be described by continuum equations.

As an example, figure 1 shows different ranges of frequency and droplet radius a, over which, in accordance with estimates, different components of the total interaction force predominate; in particular the ranges over which the quasi-stationary force f_μ, viscosity forces (f_μ,f_{B}) and inertial forces (f_m,f_A) are dominant.

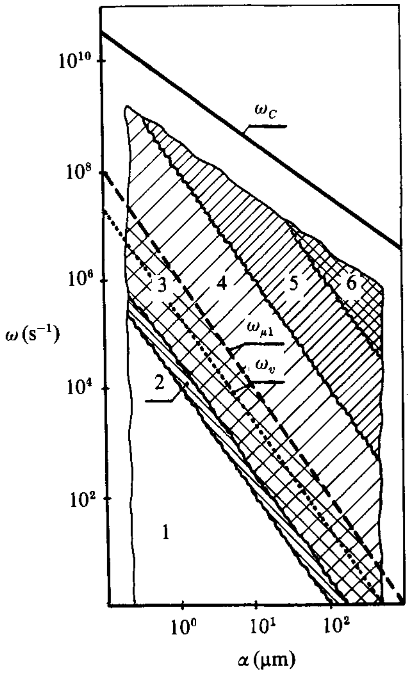

FIGURE 1. A diagram illustrating possible regimes of force interaction between vapour and droplets of various radii a under an acoustic field with frequency ω. In the regions marked 1–6 the following forces dominate: 1, f_μ (phases are in velocity equilibrium owing to f_μ, $u_1 = u_2$); 2, f_μ ($u_1 \neq u_2$); 3, $f_\mu + f_B$; 4, $f_\mu + f_B + f_m + f_A$; 5, $f_B + f_m + f_A$; 6, $f_m + f_A$.

The solid and dashed lines trace the above-described characteristic frequencies ω_C and $\tau_{\mu1}^{-1}$, and the dash–dotted line traces the frequency $\omega_v = \tau_v^{-1}$ (see (11)). The computations are carried out for a saturated mixture of water vapour and droplets at $p = 1.0$ MPa.

The expression for the main part of the interfacial force depending upon the relative velocity of the phases $u_{12} = u_1 - u_2$ can be written in the form

$$\left.\begin{aligned} f_{\mu Bm} &= f_\mu + f_B + f_m = K^* u_{12}, \\ \frac{K^*}{K_\mu} &= 1 + \frac{1-i}{\sqrt{2}}(\omega\tau_{\mu1})^{\frac{1}{2}} - \frac{1}{9}i\omega\tau_{\mu1}; \quad K_\mu = 6\pi a \mu_1. \end{aligned}\right\} \qquad (10)$$

Here K^* is a frequency-dependent complex drag coefficient which characterizes the interfacial momentum transfer under the unsteady laminar flow around a particle. The fact that K^* is complex indicates that there is a phase shift between oscillations of the force $f_{\mu Bm}$ and those of the slip velocity u_{12}. The interfacial force $f_{\mu Bm}$ is determined by the absoslute value $K = |K^*|$, the phase shift by the principal value of the argument $\varphi = |\arg K^*|$.

Figure 2 illustrates how K and φ depend on ω. Clearly, the drag coefficient strongly depends on frequency; at dimensionless frequencies $\omega\tau_{\mu1} > 100$ it is at least an order of magnitude greater than the ordinary Stokes drag coefficient K_μ. The effect of virtual mass on K^* becomes appreciable at frequencies $\omega\tau_{\mu1} \gtrsim 1$, and grows to be comparable with the Basset effect at $\omega\tau_{\mu1} \sim 100$. The phase shift φ increases with increasing frequency, and $\varphi \to \frac{1}{2}\pi$ as $\omega \to \infty$. (This limit is a result of virtual mass effects, since the Basset memory effect gives $\varphi \to \frac{1}{4}\pi$ as $\omega \to \infty$.)

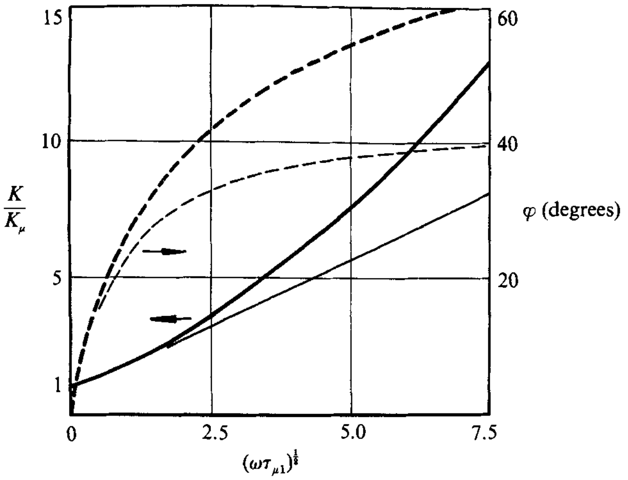

FIGURE 2. Dimensionless drag coefficient K/K_μ (solid curves) and phase shift φ between the oscillations of force and slip velocity (dashed curves) as functions of frequency. The lower thin curves plot the corresponding functions when only the Basset effect is taken into account.

Let us introduce a complex relaxation time for momentum transfer between phases under acoustic perturbations. With that end in view, the momentum equation of the dispersed phase may be written in the form

$$\left.\begin{aligned}\frac{\partial u_2}{\partial t} = \frac{nf}{\rho_2} = \frac{u_1-u_2}{\tau_v^*} - \frac{u_1}{\tau_A^*},\\ \tau_v^* = \tau_v\frac{K_\mu}{K^*},\quad \tau_A^* = -\frac{\rho_2^0}{\rho_1^0}\frac{\mathrm{i}}{\omega},\quad \tau_v = \frac{2}{9}\frac{\rho_2^0 a^2}{\mu_1};\quad \tau_v \gg \tau_{\mu 1}\quad (\rho_2^0 \gg \rho_1^0).\end{aligned}\right\} \qquad (11)$$

Here τ_v is the ordinary dynamic relaxation time under steady Stokes flow of gas around a particle; τ_v^* is its complex analogue; τ_A^* denotes the complex time characterizing the change of particle momentum due to the unsteady buoyancy force; K^* and K_μ are the drag coefficients introduced above (see (10)).

Note that two-velocity effects are of no importance at $\omega < 10^{-1}/\tau_v$. In this case the velocities of both phases are practically identical ($u_1 \approx u_2$), owing to the viscous Stokes force (see figure 2).

2.3. *Non-stationary effects of interfacial heat and mass transfer*

The gas Prandtl number is $Pr_1 \sim 1$; therefore the characteristic time $\tau_{\lambda 1} = a^2/\kappa_1$ of the build-up of the quasi-stationary thermal field within the gas around a droplet is of the same order of magnitude as the characteristic time $\tau_{\mu 1}$. Consequently, the transient nature of temperature fields around particles or droplets, resulting in frequency dependence of the interfacial heat and mass transfer intensity, manifests itself at the same acoustic frequencies as the transient nature of velocity fields, resulting in the frequency dependence of the interfacial force.

The temperature conductivity of the condensed phase κ_2 is usually much smaller than that of the gas κ_1 ($\kappa_2 \ll \kappa_1$), hence the characteristic time $\tau_{\lambda 2} = a^2/\kappa_2$ of the build-up of the quasi-stationary (uniform) thermal field within the droplet is much greater than that within the gas ($\tau_{\lambda 2} \gg \tau_{\lambda 1}$). As a result, the transient heat transfer from the surface of the droplet to the liquid inside it, leading to a frequency dependence of heat flux $q_{2\sigma}$, seems to be appreciable even at lower acoustic frequencies than the effect of transient heat transfer to the gas†.

Within the framework of the accepted three-temperature scheme of the interfacial heat and mass transfer (2), the continuous distribution of microtemperatures T' inside and outside each individual droplet is replaced by the following step distribution function:

$$T'(r) = \begin{cases} T_2, & r < a, \\ T_\sigma, & r = a, \\ T_1, & r > a, \end{cases}$$

where T_1 and T_2 are the characteristic macrotemperatures of the gas and the droplets respectively, and T_σ is the temperature of the droplet surface.

The true values of the heat fluxes $q_{1\sigma}$ and $q_{2\sigma}$ are governed by the actual frequency-dependent distributions of microtemperatures in the continuous and dispersed phases. To obtain proper relationships let us consider (in a reference frame fixed to the centre of a particle of the dispersed phase) the problem of heat transfer between a spherical particle and the gas. In a monochromatic acoustic wave with driving frequency ω we have

$$(T'_j(r,t) - T_0),\ (p(t) - p_0) \sim \exp(-\mathrm{i}\omega t).$$

The heat-influx equations for the external (outside the particle) and internal (inside the particle) regions in the case of the spherically symmetrical problem are

$$\left.\begin{aligned} \frac{\partial T'_1}{\partial t} &= \kappa_1 \left(\frac{\partial^2 T'_1}{\partial r^2} + \frac{2}{r}\frac{\partial T'_1}{\partial r}\right) + \frac{1}{\rho^0_{10} c_1}\frac{\partial p(t)}{\partial t}, \\ \frac{\partial T'_2}{\partial t} &= \kappa_2 \left(\frac{\partial^2 T'_2}{\partial r^2} + \frac{2}{r}\frac{\partial T'_2}{\partial r}\right). \end{aligned}\right\} \tag{12}$$

The boundary conditions for (12) have the form

$$T'_1(a,t) = T'_2(a,t) = T_\sigma(t), \quad \left.\frac{\partial T'_1}{\partial r}\right|_{r\to\infty} = 0, \quad \left.\frac{\partial T'_2}{\partial r}\right|_{r=0} = 0.$$

The solutions of these problems in the case of monochromatic waves are well-known;

$$\left.\begin{aligned} T'_1(r) - T_\infty &= A_1 \frac{a}{r} \exp\left\{-(1-\mathrm{i})\left(\frac{\omega}{2\kappa_1}\right)^{\frac{1}{2}} r\right\}, & r &\geqslant a, \\ T'_2(r) - T_0 &= A_2 \frac{a}{r} \sinh\left\{(1-\mathrm{i})\left(\frac{\omega}{2\kappa_2}\right)^{\frac{1}{2}} r\right\}, & r &\leqslant a, \end{aligned}\right\} \tag{13}$$

where A_1 and A_2 are constants which can be determined by the boundary conditions at the interface, and T_∞ is the temperature far from the droplet.

Consider a cell of radius $R = a/\alpha_2^{\frac{1}{3}}$ around a particle of radius a. Integrating the

---

† The more detailed analysis given below demonstrates that the transient behaviour of the temperature field affects the intensity of heat transfer within a droplet even at higher frequencies than in the gas outside it, in spite of $\tau_{\lambda 2} \gg \tau_{\lambda 1}$.

distributions (13) over the masses of the phases in the cell when $\alpha_2^{\frac{1}{3}} \ll 1$, we can find the complex amplitudes of the mass-averaged temperatures of the phases:

$$\left.\begin{aligned} &T_1 = T_\infty, \quad T_2 = \frac{3}{a^3}\int_0^a T_2'(r)\, r^2\, \mathrm{d}r = 3A_2 \frac{z_2 \cosh z_2 - \sinh z_2}{z_2^2} + T_0', \\ &z_j = \frac{1-\mathrm{i}}{\sqrt{2}}(\omega\tau_{\lambda j})^{\frac{1}{2}}, \quad \tau_{\lambda j} = \frac{a^2}{\kappa_j}, \quad j = 1, 2. \end{aligned}\right\} \tag{14}$$

Let us take into consideration the dimensionless complex parameters of heat transfer Nu_j^*, the so-called complex 'Nusselt numbers'

$$Nu_j^* = \frac{q_{j\sigma}}{2\pi a \lambda_j (T_j - T_\sigma)},$$

$$q_{1\sigma} = 4\pi a^2 \lambda_1 \left.\frac{\partial T_1'}{\partial r}\right|_{r=a}, \quad q_{2\sigma} = -4\pi a^2 \lambda_2 \left.\frac{\partial T_2'}{\partial r}\right|_{r=a},$$

where λ_j is the thermal conductivity of the jth phase ($j = 1, 2$).

Using the temperature distributions (13), the mass-averaged temperature (14), and the above definitions, we may write down the following expressions for these parameters:

$$\left.\begin{aligned} &Nu_1^*(\omega) = \frac{2}{\eta_1(z_1)}, \quad Nu_2^*(\omega) = \frac{10}{\eta_2(z_2)}, \\ &\eta_1(z_1) = \frac{1}{1+z_1}, \quad \eta_2(z_2) = \frac{5[3z_2 - (3+z_2^2)\tanh z_2]}{z_2^2(\tanh z_2 - z_2)}, \quad |\eta_1|, |\eta_2| \leqslant 1. \end{aligned}\right\} \tag{15}$$

The formula for $Nu_2^*(\omega)$ is substantially more complicated than that for $Nu_1^*(\omega)$, and it is useful to give simpler expressions for $Nu_2^*(\omega)$ which are valid for some frequency ranges:

$$\left.\begin{aligned} &Nu_2^*(\omega) \approx 10(1+\tfrac{1}{35}z_2^2) = 10\left[1 - \frac{\mathrm{i}}{35}\omega\tau_{\lambda 2}\right], && |z_2|^4 = (\omega\tau_{\lambda 2})^2 \ll 1, \\ &Nu_2^*(\omega) \approx \frac{2z_2(z_2-1)}{z_2^2 - 3(z_2-1)}, && |z_2| = (\omega\tau_{\lambda 2})^{\frac{1}{2}} > 2, \\ &Nu_2^*(\omega) \approx 2z_2 = \sqrt{2}(1-\mathrm{i})\,(\omega\tau_{\lambda 2})^{\frac{1}{2}}, && |z_2|^2 = (\omega\tau_{\lambda 2}) \gg 1. \end{aligned}\right\} \tag{16}$$

An important feature of the above low-frequency $Nu_2^*(\omega)$ asymptotics is a weak linear dependence of the imaginary part on ω, and the constancy of the real part. The high-frequency asymptotics for $Nu_2^*(\omega)$ coincide with the corresponding asymptotics for $Nu_1^*(\omega)$, because thermal boundary layers at high frequencies are extremely thin and the difference between the internal and external thermal problems disappears.

The heat transfer coefficients Nu_j^* are complex, and this points to a phase shift between the oscillations of heat fluxes and those of temperature differences $(T_j - T_\sigma)$. The intensities of heat fluxes are determined by the absolute values $Nu_j = |Nu_j^*|$, and phase shifts by the principal values of arguments $\varphi_j = |\arg Nu_j^*|$.

Curves plotting $Nu_j(\omega)$ and $\varphi_j(\omega)$ are shown in figure 3. Clearly, as $\omega \to 0$, we have $Nu_2 \to 10$ while $Nu_1 \to 2$. The heat transfer coefficient Nu_1 is close to its stationary value $Nu_1 = 2$ only if $\omega < 10^{-2}\tau_{\lambda 1}^{-1}$. As for the parameter Nu_2, the coefficient $\frac{1}{35}$ in the low-frequency asymptotics (16) is so small that Nu_2 is practically indistinguishable from its quasi-stationary value $Nu_2 = 10$, even at $\omega \sim 10\tau_{\lambda 2}^{-1}$. Correspondingly, a small phase shift φ_1 is observed only at $\omega < 10^{-2}\tau_{\lambda 1}^{-1}$, while φ_2 is nearly zero even at $\omega \sim 10\tau_{\lambda 2}^{-1}$. Note that $\tau_{\lambda 1}/\tau_{\lambda 2} = \kappa_2/\kappa_1$, and that in mixtures of gas–particle type this

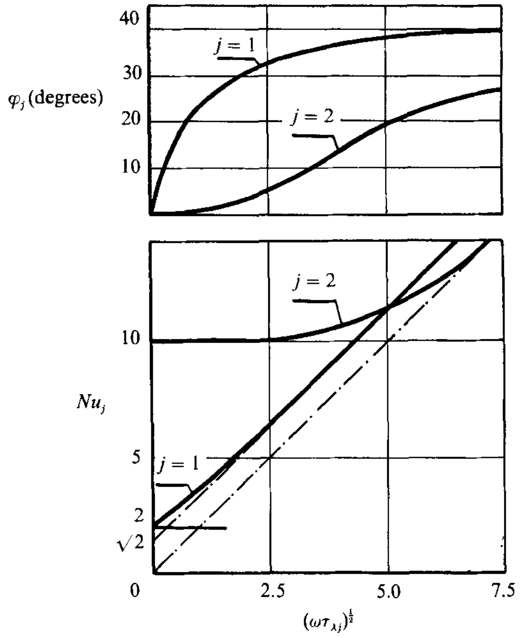

FIGURE 3. Heat transfer parameters Nu_j (Nusselt numbers) and phase shifts φ_j between oscillations of heat fluxes and temperature differences as functions of characteristic dimensionless frequencies ($j = 1, 2$).

quantity is of order 10^{-1}–10^{-2}. As a result, even though $\tau_{\lambda 2} \gg \tau_{\lambda 1}$, the 'internal' nonstationarity begins to affect the intensity of heat transfer between phases at higher frequencies of acoustic perturbations than the 'external' one.

Let us introduce the concept of the complex times of temperature relaxation in individual phases; for this purpose it is instructive to rewrite the formulae for the 'external' ($q_{1\sigma}$) and 'internal' ($q_{2\sigma}$) heat fluxes to the droplet surface in the forms

$$\frac{nq_{1\sigma}}{\alpha_1 \rho_1^0 c_1} = \frac{T_1 - T_\sigma}{\tau_{T1}^*}, \quad \frac{nq_{2\sigma}}{\alpha_2 \rho_2^0 c_2} = \frac{T_2 - T_\sigma}{\tau_{T2}^*}, \tag{17}$$

$$\tau_{T1}^* = \frac{1}{3}\frac{\alpha_1}{\alpha_2}\tau_{\lambda 1}\,\eta_1(z_1), \quad \tau_{T2}^* = \tfrac{1}{15}\tau_{\lambda 2}\,\eta_2(z_2). \tag{18}$$

Here τ_{Tj}^* is the complex temperature relaxation time in the jth phase, determined by a characteristic time $\tau_{\lambda j}$ and frequency ω. As follows from (15), (16), complex relaxation times τ_{Tj}^* are close to their quasi-stationary real values τ_{Tj} at low frequencies, different for each individual phase,

$$\tau_{T1}^* \approx \tau_{T1} = \frac{1}{3}\frac{\alpha_1}{\alpha_2}\tau_{\lambda 1}, \quad \omega\tau_{\lambda 1} < 10^{-2}, \quad |\eta_1| \sim 1,$$

$$\tau_{T2}^* \approx \tau_{T2} = \tfrac{1}{15}\tau_{\lambda 2}, \quad \omega\tau_{\lambda 2} < 1, \quad |\eta_2| \sim 1.$$

In the case of a phase transformation at the surface of a droplet, the surface temperature T_σ is determined by the phase transformation rate. The process obeys the well-known Herz–Knudsen–Langmuir formula that we write in the form

$$\frac{njl}{\alpha_2 \rho_1^0 c_1} = \frac{T_s - T_\sigma}{\tau_\sigma}, \quad \tau_\sigma = \frac{1 - \rho_1^0/\rho_2^0}{3(\gamma_1 - 1)}\left(\frac{2\pi}{\gamma_1}\right)^{\frac{1}{2}}\frac{aC_1^3}{\beta l^2}, \tag{19}$$

where τ_σ is the 'relaxation time' of temperature at the interface, depending on the accommodation coefficient β and independent of frequency ω; T_s is the saturation temperature, which is a known function of pressure. In the case of small perturbations along the saturation curve, the following Clapeyron–Clausius relationship holds:

$$\mathrm{d}T_s = \frac{\mathrm{d}T_s}{\mathrm{d}p}\mathrm{d}p, \quad \frac{\mathrm{d}T_s}{\mathrm{d}p} = \frac{T_0(1-\rho_1^0/\rho_2^0)}{l\rho_1^0}.$$

Although the characteristic time τ_σ is independent of ω, the rate of the phase transition j does depend on frequency ω, because frequency affects heat fluxes $q_{j\sigma}$ towards the interface (these fluxes account for the in- or outflow of heat absorbed or released in evaporation or condensation respectively).

2.4. *Comparative evaluation of characteristic times and temperature differences*

In order to compare the characteristic temperature differences $T_1 - T_\sigma$, $T_2 - T_\sigma$ and $T_\sigma - T_s$ arising in acoustically perturbed vapour–droplet mixtures, we make use of the equation of heat inflow to the interface, $q_{1\sigma} + q_{2\sigma} = -jl$ (see (2)). It yields

$$\left.\begin{gathered} \frac{T_1 - T_\sigma}{\tau^*_{1\sigma}} = \frac{T_\sigma - T_2}{\tau^*_{2\sigma}} + \frac{T_\sigma - T_s}{\tau_\sigma}, \\ \tau^*_{1\sigma} = \frac{\alpha_2}{\alpha_1}\tau^*_{T1} = \tfrac{1}{3}\tau_{\lambda 1}\,\eta_1(z_1), \quad \tau^*_{2\sigma} = \frac{\rho_1^0 c_1}{\rho_2^0 c_2}\tau^*_{T2} = \frac{\rho_1^0 c_1 a^2}{15\lambda_2}\eta_2(z_2). \end{gathered}\right\} \tag{20}$$

Here $\tau^*_{1\sigma}$ and $\tau^*_{2\sigma}$ are the characteristic complex times necessary to equalize the corresponding temperature differences in (20). The left-hand side of this equation is proportional to the heat flux from the gas to the interface; this flux provides the heat consumed by the phase transition (the second term on the right) and is required to change the temperature of the particles (the first term on the right).

A comparison of the characteristic times $\tau^*_{1\sigma}$, $\tau^*_{2\sigma}$ and τ_σ appearing in (20) shows that differences between them are usually large, and the following estimates hold:

$$\left.\begin{gathered} \frac{|\tau^*_{2\sigma}|}{|\tau^*_{1\sigma}|} = \frac{1}{5}\frac{\lambda_1}{\lambda_2}\frac{|\eta_2|}{|\eta_1|}, \quad \frac{\tau_\sigma}{|\tau^*_{2\sigma}|} \sim \frac{15}{\beta}\frac{\lambda_2}{\lambda_1}\left(\frac{C_1^2}{l}\right)^2\left(\frac{L}{a}\right)\frac{1}{|\eta_2|}, \\ (L \sim \lambda_1/(\rho_1^0 c_1 C_1) \ll a, \quad |\eta_2| \leqslant |\eta_1|; \quad |\eta_2|, |\eta_1| \leqslant 1). \end{gathered}\right\} \tag{21}$$

Here L is the mean free path of molecules in the gas. As a rule $\lambda_2 \gg \lambda_1$ and, regardless of frequency (taking into account the inequality $|\eta_2| \leqslant |\eta_1|$), we have $|\tau^*_{2\sigma}|/|\tau^*_{1\sigma}| \ll 1$. The ratio $\tau_\sigma/|\tau^*_{2\sigma}|$ can be small only within certain ranges of particle sizes and frequencies, depending upon the physical properties of the particles. Thus, for a water mixture of saturated vapour with droplets at $p = 1.0$ MPa, when $\lambda_2/\lambda_1 \approx 20$, $l/C_1^2 \approx 8$, $L \sim 10^{-8}$ m, we have

$$\frac{\tau_\sigma}{|\tau^*_{2\sigma}|} \sim \frac{10^2}{|\eta_2|}\left(\frac{L}{a}\right).$$

If the typical droplet size is $a \sim 10^{-5}$ m, then τ_σ for this mixture is much less than $|\tau^*_{2\sigma}|$ only if $|\eta_2| \sim 1$, i.e. if the 'internal' heat transfer proceeds under quasi-stationary conditions ($\omega \ll \tau_{\lambda 2}^{-1}$).

The heat inflow equation (20), taken together with estimates (21), leads to the conclusion that the temperature non-uniformity within droplets ($T_2 \neq T_\sigma$) is small compared with that in the gas phase (deviations of T_1 from T_σ). A non-equilibrium at the interfaces (deviation T_σ from T_s) can be observed only at high acoustic frequencies and small sizes of droplets, as in these cases $|\tau^*_{2\sigma}|$ becomes small and tends to τ_σ because of small values of $|\eta_2|$ or a. The following estimates for characteristic temperature differences in vapour–droplet mixtures are typical:

$$|T_\sigma - T_s| \ll |T_\sigma - T_2| \ll |T_1 - T_\sigma|.$$

If no phase transition occurs, the equation of heat inflow to the particle surface takes the form

$$q_{1\sigma} + q_{2\sigma} = 0 \quad \text{or} \quad \frac{T_1 - T_\sigma}{\tau^*_{1\sigma}} + \frac{T_2 - T_\sigma}{\tau^*_{2\sigma}} = 0.$$

This equation enables us to eliminate T_σ from the equation (2) for heat influx to the particles and rewrite it in the form

$$\left.\begin{aligned} &\frac{\partial T_2}{\partial t} = \frac{T_1 - T_2}{\tau^*_T}, \quad \tau^*_T = \frac{\rho^0_2 c_2}{\rho^0_1 c_1}(\tau^*_{1\sigma} + \tau^*_{2\sigma}), \\ &\tau^*_T \approx \tau^*_{1\sigma}\frac{\rho^0_2 c_2}{\rho^0_1 c_1} = \tau_T\, \eta_1(z_1), \quad \tau_T = \frac{\rho^0_2 c_2 a^2}{3\lambda_1}. \end{aligned}\right\} \tag{22}$$

Here τ_T is the ordinary 'quasi-stationary' time of temperature relaxation between phases, and τ^*_T is its complex analogue. In this approximate expression for τ^*_T we have taken into account the first estimate of (21), which implies that for $\lambda_2 \gg \lambda_1$ and for no phase transformations at the droplet surface the non-stationary character of the 'internal' heat transfer is unimportant, regardless of frequency.

3. Dispersion and absorption of perturbations in vapour–droplet and gas–particle mixtures

The system of linear equations (1)–(3), (11), (15), (17) and (19) is closed. It can be used over a wide range of frequencies to analyse the propagation of small perturbations in mixtures of vapour or gas with liquid or solid particles, both with or without phase transitions on interfaces. We now proceed to solve the system and to analyse its travelling-wave solutions (4). For convenience the following dimensionless parameters characterizing the composition of the mixture and the physical properties of the individual phases will be used:

$$m = \frac{\rho_2}{\rho_1}, \quad r = \frac{\rho^0_1}{\rho^0_2}, \quad m^0 = \frac{\rho^0_2}{\rho^0_1}, \quad \bar{c}_1 = \frac{c_1}{\gamma_1 R_1} = \frac{1}{\gamma_1 - 1}, \quad \bar{c}_2 = \frac{c_2}{\gamma_1 R_1}, \quad \bar{l} = \frac{l}{C^2_1}. \tag{23}$$

Here m is the relative mass concentration of droplets (particles) in the mixture, r is the gas-to-droplet density ratio (at moderately high pressures $r \ll 1$) and R_1 is the gas constant.

3.1. *Dispersion equations*

The dispersion equation connecting wavenumber k_* and perturbation frequency ω can be derived from the condition of the existence of a non-zero solution of the type (4) for the system of linear equations considered. It has the following form:

$$(C_1 k_*/\omega)^2 = V(\omega)\,\Theta(\omega), \tag{24}$$

$$V(\omega) = 1+m\frac{W_1-W_2}{W_3+mW_2}, \quad \Theta(\omega) = 1+m\frac{\Pi_1+(\gamma_1-1)\,\Pi_2}{\Pi_3+m\Pi_2},$$

$$W_1 = (1-\alpha_2)(1-r), \quad W_2 = r[1-r(\mathrm{i}\omega\tau_v^*)], \quad W_3 = 1-\mathrm{i}\omega\tau_v^*,$$

$$\Pi_1 = \frac{1-r}{\bar{l}^2}\left\{(1-r)(\bar{c}_1+m\bar{c}_2)-2\bar{l}-m^0\bar{c}_2(\mathrm{i}\omega\tau_{1\sigma}^*)\left[1-r+[1-r-2(\gamma_1-1)\,\bar{l}]\frac{\tau_{2\sigma}^*}{\tau_{1\sigma}^*}\right]\right\},$$

$$\Pi_2 = 1-(\mathrm{i}\omega\tau_{T2}^*)\left(1+\frac{\tau_\sigma}{\tau_{2\sigma}^*}\right),$$

$$\Pi_3 = -m^0(\mathrm{i}\omega\tau_{1\sigma}^*)\left\{1+\frac{\tau_\sigma}{\tau_{1\sigma}^*}-(\mathrm{i}\omega\tau_{T2}^*)\left[1+\frac{\tau_\sigma}{\tau_{2\sigma}^*}\left(1+\frac{\tau_{2\sigma}^*}{\tau_{1\sigma}^*}\right)\right]\right\}.$$

Here $V(\omega)$ and $\Theta(\omega)$ are complex functions depending upon the volume concentration α_2 of the condensed phase, particle size a, and thermophysical properties of the phases $(\gamma_1, C_1, l, \beta, \mu_1, \rho_j^0, c_j, \lambda_j; j = 1, 2)$. These functions describe dispersive and dissipative effects due to the relative slip of phases and the non-equilibrium interfacial heat and mass transfer respectively. If no droplets or particles are suspended ($m = 0$), these effects vanish, and $V = \Theta = 1$.

According to the estimates (21), $|\tau_{2\sigma}^*|/|\tau_{1\sigma}^*| \ll 1$ regardless of frequency, so that the terms for Π_1 and Π_3 containing this ratio can be, as a rule, neglected. The effect of non-equilibrium phase transitions becomes appreciable when the ratio $\tau_\sigma/\tau_{2\sigma}^*$, which increases with increasing frequency ω, becomes comparable with unity $(\tau_\sigma/|\tau_{2\sigma}^*| \sim 1)$.

Note that (24) is justifiable if $\alpha_2 \ll 1$. At $r \ll 1$ and $m \sim 1$ the function $V(\omega)$ and the term $\Pi_1(\omega)$ in the function $\Theta(\omega)$ are close to the functions $V^0(\omega)$ and $\Pi_1^0(\omega)$ respectively $(V(\omega) = V^0(\omega)(1+\epsilon_V(\omega)\,O(\alpha_2)),\ \Pi_1(\omega) = \Pi_1^0(\omega)(1+\epsilon_\Pi(\omega)\,O(\alpha_2))$, where $|\epsilon_V(\omega)| \leqslant 1, |\epsilon_\Pi(\omega)| \leqslant 1$ regardless of frequency). Here

$$\left.\begin{aligned} V^0(\omega) &= 1+\frac{m}{1-\mathrm{i}\omega\tau_v^{*0}}, \quad \tau_v^{*0} = \tau_v[1+\tfrac{3}{2}(1-\mathrm{i})(r\omega\tau_v)^{\frac{1}{2}}]^{-1}, \\ \Pi_1^0 &= \frac{1}{\bar{l}^2}\left\{\bar{c}_1+m\bar{c}_2-2\bar{l}-m^0\bar{c}_2(\mathrm{i}\omega\tau_{1\sigma}^*)\left[1+(1-2(\gamma_1-1)\,\bar{l})\frac{\tau_{2\sigma}^*}{\tau_{1\sigma}^*}\right]\right\}. \end{aligned}\right\} \tag{25}$$

An expression for $V(\omega)$ in the form (25) can be obtained from the governing equations directly if the buoyancy and virtual mass forces are negligible. Thus, although the absolute values of these forces are comparable with Stokes and Basset forces at high frequencies (see (9)), their contributions to dispersion and absorption of sound are small because of a phase shift between oscillations of the force and those of the velocity.

The dispersion equation describing the propagation of small perturbations in gas–particle mixtures in the absence of phase transformations (e.g. in a gas with suspended solid particles) can be derived from (24) by a limit transition $\tau_\sigma \to \infty$. In this case the function $V(\omega)$ remains the same, while $\Theta(\omega)$ transforms to the following simple form:

$$\left.\begin{aligned} \Theta(\omega) &= \frac{\gamma_1(1+m)\,c_V/c_1-\mathrm{i}\omega\tau_T^*}{\gamma_{\mathrm{e}}(1+m)\,c_V/c_1-\mathrm{i}\omega\tau_T^*}, \\ c_V = \frac{c_1-R_1+mc_2}{1+m}, &\quad c_P = \frac{c_1+mc_2}{1+m}, \quad \gamma_{\mathrm{e}} = \frac{c_P}{c_V}. \end{aligned}\right\} \tag{26}$$

Here c_V and c_P are the equilibrium specific heats at constant volume and pressure respectively, and γ_{e} is the equilibrium adiabatic exponent of a two-phase mixture without phase transformations. In writing (26), we used the complex relaxation time of temperature between phases τ_T^* discussed earlier (see (22)). The dispersion equations (24), (26) at sufficiently low frequencies $\omega < 10^{-2}\tau_{\mu 1}^{-1}$ are simpler (see Ivandaev 1978).

3.2. *Equilibrium and frozen speeds of sound*

The expressions for the equilibrium C_{e} and frozen C_{f} speeds of sound in a vapour–droplet mixture, derived from the dispersion equation (24) with $V(\omega)$ and $\Pi_1(\omega)$ from (25), by limit transitions $\omega \rightarrow 0$ and $\omega \rightarrow \infty$, can be written in the form

$$\left.\begin{aligned} C_{\mathrm{e}} = C_1\left[\frac{\gamma_{\mathrm{e}}}{\gamma_1(1+m)}\right]^{\frac{1}{2}}, &\quad C_{\mathrm{f}} = C_1, \\ \gamma_{\mathrm{e}} = \left[1+\frac{1}{\gamma_1\,\bar{l}^2}(\bar{c}_1+m\bar{c}_2-2\bar{l})\right]^{-1}&. \end{aligned}\right\} \tag{27}$$

Here γ_{e} is an analogue of the equilibrium adiabatic exponent for a two-phase mixture with phase transformations. In the particular case of no condensed phase ($m = 0$) the exponent $\gamma_{\mathrm{e}} = \gamma_{\mathrm{e}1}$ determines the speed of sound in vapour $C_{\mathrm{e}1}$, called the equilibrium speed of sound on the boundary of the two-phase region (the speed that could exist if the vapour temperature T_1 in the wave were equal to the saturation temperature T_{s} ($T_1 \equiv T_{\mathrm{s}}(p)$)):

$$C_{\mathrm{e}1} = \left(\frac{\gamma_{\mathrm{e}1}\,p}{\rho_1^0}\right)^{\frac{1}{2}}, \quad \gamma_{\mathrm{e}1} = \left[1-\frac{2}{\gamma_1\,\bar{l}}+\frac{1}{\gamma_1(\gamma_1-1)\,\bar{l}^2}\right]^{-1}.$$

The formulae for the equilibrium and frozen speeds of sound in gas–solid particle mixtures without phase transitions can be obtained by letting $\omega \rightarrow 0$ and $\omega \rightarrow \infty$ in the dispersion equation (24), with $V(\omega)$ obtained from (25) and $\Theta(\omega)$ from (26). They have the same form as (27), but with γ_{e} obtained from (26).

Note that the frozen speed of sound C_{f} can in practice be achieved ($C_{\mathrm{p}}(\omega) \approx C_{\mathrm{f}}$) at high ($\omega \gg \tau_v^{-1}, \tau_T^{-1}$), but nevertheless admissible for the continuum theory, frequencies ($\omega \ll \omega_C$).

3.3. *Analysis of sound speed and attenuation coefficient dependence upon frequency*

It would hardly be meaningful to give here the explicit formulae describing the dependences of the phase C_{p} and group C_{g} speeds and the linear k_{**} and dimensionless σ attenuation coefficients upon frequency ω and thermodynamic parameters of the mixture: they are very unwieldy. The dependences can be analysed by examining the results of direct calculations. The calculations, partly illustrated below, were carried out for a monodisperse vapour–water mixture of droplet structure ($\alpha_2 < 0.05$), at initial pressure $p = 1.0$ MPa. The range of frequency where the condition of acoustic homogeneity is valid ($L_\omega \sim k^{-1} \gg a$) was considered.

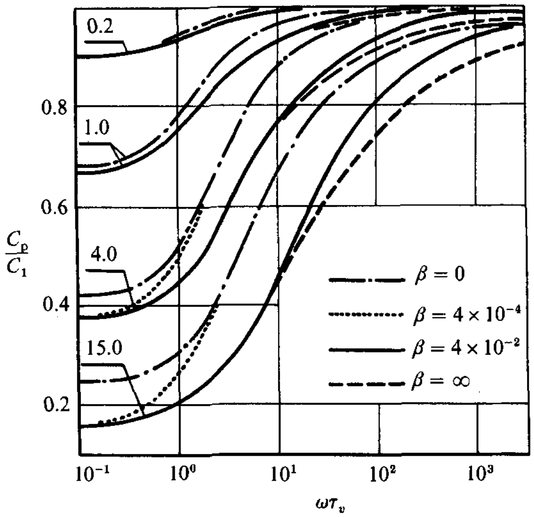

FIGURE 4. Dimensionless phase velocity C_p/C_l of weak harmonic perturbations propagating through a saturated mixture of water vapour and droplets at a pressure $p = 1.0$ MPa, as a function of dimensionless frequency $\omega\tau_v$. Numbers marking different series of curves show the relative mass concentration m of droplets in the mixture. Each curve within a series corresponds to a particular value of the accommodation coefficient β.

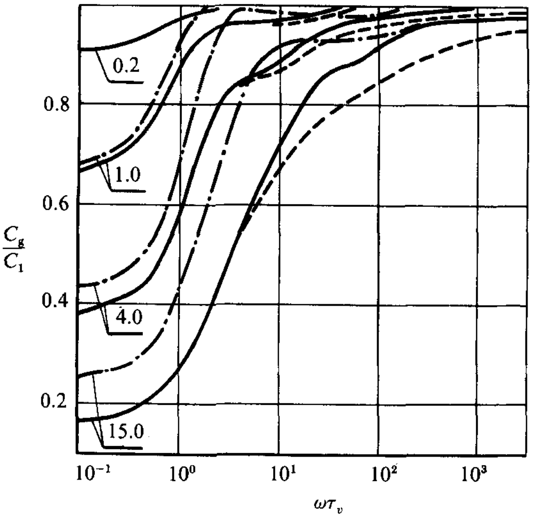

FIGURE 5. Dimensionless group velocity C_g/C_l of weak harmonic perturbations propagating in a mixture of water vapour and droplets at a pressure $p = 1.0$ MPa, as a function of dimensionless frequency $\omega\tau_v$. For description of curves, see figure 4.

Selected results of the calculations are plotted in figures 4–7. Each series of curves in the figures corresponds to a definite mass concentration of the condensed phase. Each curve within a series corresponds to a definite value of the accommodation coefficient β. Solid curves correspond to $\beta = 0.04$, sometimes recommended for water (note that for $p = 1.0$ MPa $(T = T_s(p))$, for $a = 30$ μm, and for $\beta = 0.04$ we have $\tau_\sigma/\tau_v = 6 \times 10^{-6}$); the other curves illustrate the effect of β upon dispersion and attenuation of perturbations. The case $\beta = 0$ is that of frozen mass transfer $(\tau_\sigma = \infty)$

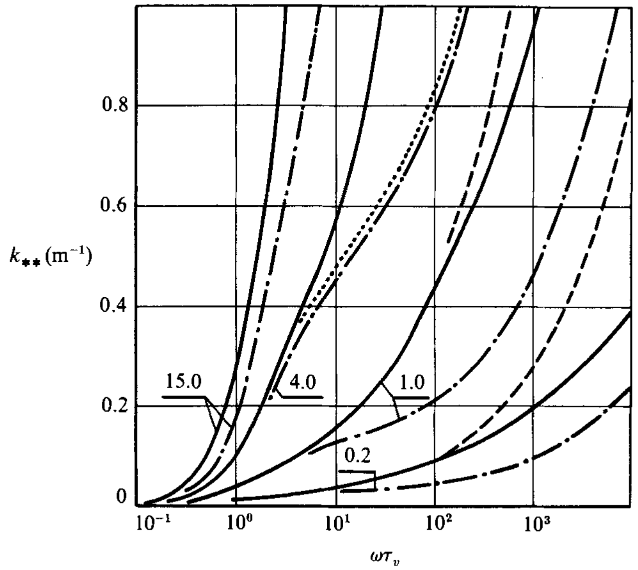

FIGURE 6. Linear attenuation coefficient k_{**} of weak harmonic perturbations propagating through a mixture of water vapour and droplets at a pressure $p = 1.0$ MPa, as a function of dimensionless frequency $\omega\tau_v$. For description of curves, see figure 4.

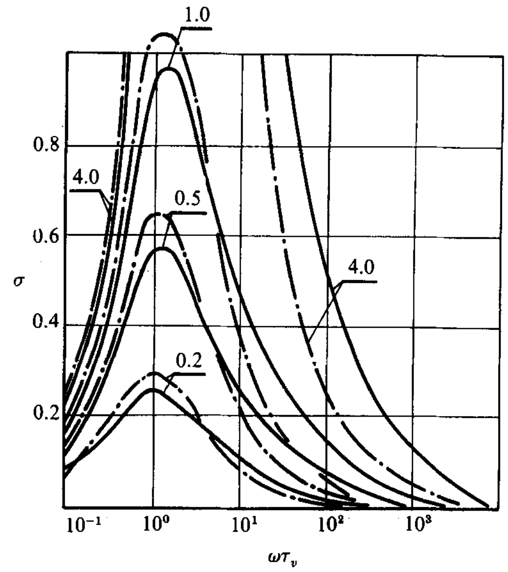

FIGURE 7. Dimensionless attenuation coefficient per wavelength σ as a function of dimensionless frequency $\omega\tau_v$ for weak harmonic perturbation in a saturated mixture of water vapour and droplets ($p = 1.0$ MPa). For description of curves, see figure 4.

and the case denoted by $\beta = \infty$ is that of quasi-equilibrium mass transfer at $T_\sigma = T_s$ ($\tau_\sigma = 0$). The curves corresponding to finite values of β lie within a region bounded by the limiting curves $\beta = 0$ and $\beta = \infty$, and tend to them at high and low frequencies, respectively.

The solid curves ($\beta = 0.04$) almost coincide with the dashed curves ($\beta = \infty$) when $\tau_\sigma \ll |\tau^*_{2\sigma}|$ (see the discussion of (21)), that is up to frequencies $\omega\tau_{\lambda 2} \lesssim 10$ at which

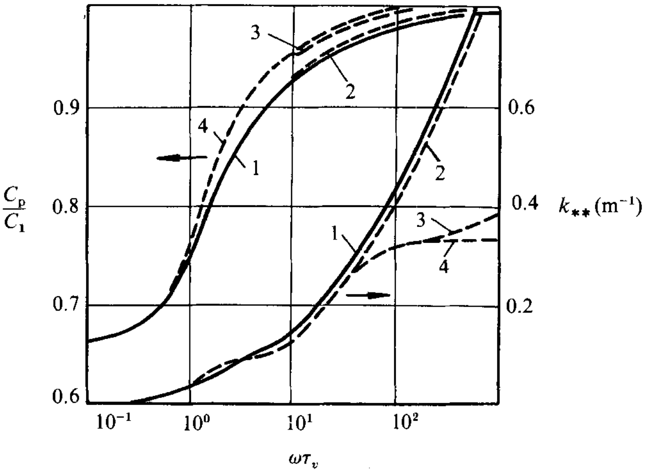

FIGURE 8. The contributions of individual non-stationary effects to dispersion and dissipation of small perturbations in a water vapour–droplet mixture at a pressure $p = 1.0$ MPa ($m^0 = \rho_2^0/\rho_1^0 = 172$). Curve 1, all non-stationary effects are taken into account; 2, only non-stationary effects of interfacial momentum transfer are taken into account; 3, only thermal non-stationary effects are taken into account; 4, non-stationary effects are neglected. The mass concentration of droplets in the mixture is $m = 1$.

$|\eta_2| \sim 1$, i.e. up to $\omega\tau_v \lesssim 10$. If we use the assumption of quasi-equilibrium mass transfer ($\beta = \infty$) at high frequencies, we reduce the phase velocity of small perturbations and enhance their linear attenuation coefficient. If the assumption of frozen mass transfer is used, the velocities are enhanced and the linear attenuation coefficient is diminished, while the attenuation coefficient per wavelength σ becomes bigger at low, and smaller at high, frequencies. The group velocity curves $C_g(\omega)$ tend to form local maxima and minima at certain frequencies which depend upon the droplet content in the mixture.

To take into account the non-stationary effects of interfacial interaction under high-frequency perturbations, we have to take into account the deviations of τ_v^*, τ_{T1}^* and τ_{T2}^* from τ_v, $\frac{1}{3}\tau_{\lambda 1}$ and $\frac{1}{15}\tau_{\lambda 2}$ respectively. The deviations occur as the boundary layers in and around droplets become thinner than those predicted by the quasi-stationary theory. Because of thin boundary layers the interfacial transfer processes proceed faster, are more in 'equilibrium' than within the framework of quasi-stationary correlations, and are shifted in phase with respect to the corresponding thermodynamic forces. As a result, owing to non-stationary effects the speed of weak perturbations decreases, while the linear attenuation coefficient increases.

Let us emphasize the following interesting observation. If we neglect non-stationary effects, the theory yields group velocities $C_g(\omega)$ that may exceed the frozen speed of sound in the mixture, C_f. Further, the linear attenuation coefficient $k_{**}(\omega) \to \text{const}$ as $\omega \to \infty$. If non-stationary effects are taken into account, $C_g(\omega) < C_f$ for the calculated cases, and $k_{**} \to \infty$ like the square root of ω as $\omega \to \infty$. The principal term of the asymptotic expression for $k_{**}(\omega)$, whose residual term is bounded, takes, as $\omega \to \infty$, the form

$$k_{**}(\omega) \sim \frac{1}{2}\frac{mr^{\frac{1}{2}}}{\tau_v C_1}\{\tfrac{3}{2} + (\gamma_1 - 1)\,Pr_1^{-\frac{1}{2}}\}(\omega\tau_v)^{\frac{1}{2}}.$$

The contribution of each individual non-stationary component of interfacial momentum and heat transfer, and its effect on the dispersion curves, is shown in figure 8. It is clear that the main non-stationary effects are the effects of interfacial drag (i.e. the effect of the Basset force, see the discussion of (25)). They become appreciably different from zero at $\omega\tau_{\mu 1} = \frac{9}{2}(\rho_1^0/\rho_2^0)\,\omega\tau_v > 10^{-2}$, in complete agreement with (9). Thermal non-stationary effects are much weaker, and become perceptible at substantially higher frequencies.

The quantities ω and a enter complex functions $V(\omega)$ and $\Theta(\omega)$, which define k_*/ω, only as dimensionless combinations $\omega\tau_{\mu 1}$, $\omega\tau_{\lambda 1}$, $\omega\tau_{\lambda 2}$ and $\omega\tau_\sigma$. They characterize the ratios of various relaxation times $(\tau_{\mu 1}, \tau_{\lambda 1}, \tau_{\lambda 2} \sim a^2;\, \tau_\sigma \sim a)$ to the period of oscillations ω^{-1}. Let us fix the properties of the phases $(\gamma_1, C_1, l, \rho_j^0, c_j;\, j = 1, 2)$ and single out two limiting cases: one of no phase transitions $(\tau_\sigma = \infty)$ and one of quasi-equilibrium at the interface $(\tau_\sigma = 0)$. In both of these cases the combination $\omega\tau_\sigma$ does not enter the dispersion relation, while all the other dimensionless combinations differ only by constant factors. This means that in these τ_σ-limiting cases the dispersion relation $k_*/\omega = f(\omega, a)$ is a function of a single complex ωa^2, i.e. of a single dimensionless parameter. We can take as such a parameter, for instance, $\bar{\omega} = \omega\tau_v$, which is the most significant for a gas–particle mixture. Hence, for $\omega\tau_\sigma \gg 1$ or $\omega\tau_\sigma \ll 1$, we have

$$C_{\mathrm{p,g}}(\omega, a) = C_{\mathrm{p,g}}(\omega a^2) = C_{\mathrm{p,g}}(\bar{\omega}); \quad \sigma(\omega, a) = \sigma(\omega a^2) = \sigma(\bar{\omega}),$$

$$\bar{\omega} = \omega\tau_v = \frac{2\rho_2^0}{9\mu_1}\,\omega a^2.$$

In other words, when phase transitions are frozen $(\beta = 0)$ or when they are quasi-equilibrium $(\beta = \infty)$, the curves $C_{\mathrm{p,g}}(\bar{\omega})$ and $\sigma(\bar{\omega})$ (dashed and dash–dotted curves in figures 4–7) are valid for arbitrary particle sizes within the admissible range $(\omega \ll \omega_C)$. Non-self-similarity of $C_{\mathrm{p,g}}(\bar{\omega})$ and $\sigma(\bar{\omega})$, i.e. an additional effect of particle size on these functions, manifests itself only under phase transitions, when there is no temperature equilibrium on interfaces and the difference between T_σ and saturation temperature T_{s} is appreciable. Such a situation occurs when $\tau_\sigma/|\tau_{2\sigma}^*| \sim 1$.

4. Conclusion

The dispersion equations derived in the paper allow us to calculate not only the dynamics of monochromatic waves, but of an arbitrary perturbation, by considering it as a superposition of monochromatic waves and using Fourier transformation.

At low mass concentrations of the dispersed phase $(m \ll 1)$, generalization of the dispersion equations for a polydisperse mixture can be found easily. Essentially, in this case, the contribution of each fraction of the particles to the dispersion and absorption of sound is proportional to its mass concentration.

The results of the reported analysis of momentum, heat and mass transfer processes between the phases of a vapour–droplet mixture in an acoustic field allow us to indicate typical frequency ranges over which some approximate schemes or theories are valid. If $\omega\tau_v \ll 1$ we can use the simplest one-velocity scheme. Two-velocity effects have to be taken into account if $\omega\tau_v \gtrsim 1$. If, besides, $(\omega\tau_{\mu 1})^{\frac{1}{2}} \ll 1$, i.e. $\omega\tau_{\mu 1} \lesssim 10^{-2}$, then interfacial momentum transfer is quasi-stationary, and the resistance force is the Stokes drag. At higher frequencies, non-stationary effects of the interfacial interaction take place, intensity of interfacial momentum transfer increases and a certain phase shift between the interfacial force and the slip velocity can be observed. These effects must be taken into account for $(\omega\tau_{\mu 1})^{\frac{1}{2}} \gtrsim 0.1$. An equilibrium one-temperature scheme can be used if $\omega\tau_T \ll 1$. Thermal non-equilibrium effects $(T_1 \neq T_2)$ must be taken into account if $\omega\tau_T \gtrsim 1$. In this non-equilibrium case, at not very high frequencies ($(\omega\tau_{\lambda 1})^{\frac{1}{2}} \ll 1$ or $\omega\tau_{\lambda 1} \lesssim 10^{-2}$) the simpler quasi-stationary scheme of heat transfer in the gas phase $(Nu_1 = 2, \varphi_1 = 0)$ can be employed. As a rule $\omega\tau_{\lambda 2} < 1$ if $\omega\tau_{\lambda 1} \lesssim 10^{-2}$, hence the quasi-stationary scheme of heat transfer in the droplet phase $(Nu_2 = 10, \varphi_2 = 0)$ is valid in the same range of ω.

Non-stationary effects of interfacial heat transfer resulting in enhanced parameters Nu_j and phase shifts φ_j between $q_{j\sigma}$ and $T_j - T_\sigma$ must be taken into account when $(\omega\tau_{\lambda 1})^{\frac{1}{2}} > 0.1$ and $\omega\tau_{\lambda 2} > 1$. Typically $\tau_{\lambda 2} \gg \tau_{\lambda 1}$, because $\kappa_2 \ll \kappa_1$. In spite of this the upper limit of frequencies at which the quasi-stationary scheme of interfacial heat transfer can be used is frequently imposed by the gas-phase properties (see figure 3).

The following four frequency ranges can thus be singled out:

$$\text{(I)} \qquad 0 \leqslant \omega \ll (\tau_v^{-1}, \tau_T^{-1}),$$

$$\text{(II)} \qquad (\tau_v^{-\frac{1}{2}}, \tau_T^{-\frac{1}{2}}) \lesssim \omega^{\frac{1}{2}} \ll (\tau_{\mu 1}^{-\frac{1}{2}}, \tau_{\lambda 1}^{-\frac{1}{2}}),$$

$$\text{(III)} \qquad \tau_{\lambda 2}^{-\frac{1}{2}} \lesssim \omega^{\frac{1}{2}} \lesssim (\tau_{\mu 1}^{-\frac{1}{2}}, \tau_{\lambda 1}^{-\frac{1}{2}}),$$

$$\text{(IV)} \qquad \tau_{\lambda 1}^{-1} < \omega \ll \omega_C.$$

The equilibrium theory is valid for range I; the non-equilibrium theory employing the approximation of quasi-stationary interfacial transfer can be used for range II, the non-equilibrium theory taking into account non-stationary effects of interfacial momentum and heat transfer in the gas phase for range III, and the general non-equilibrium theory taking into account the non-stationary effects of heat transfer within the particles of the dispersed phase for range IV.

REFERENCES

ALTBERG, W. & HOLZMAN, M. 1925 Über die Absorption des Schalles in tröen Medien. *Phys. Z.* **26**, 149–157.

BERGMANN, L. 1954 *Der Ultraschall und seine Anwendung in Wisseschaft und Technik.* Stuttgart: Hirzel.

BHUTANI, P. O. & CHANDRAN, P. 1977 Weak waves in dusty gas. *Intl J. Engng Sci.* **15**, 9–10, 537–544.

BORISOV, A. A., VAKHGELT, A. F. & NAKORYAKOV, V. E. 1980 Propagation of long-wavelength finite-amplitude perturbations in gas-particle mixtures. *Zh. Prikl. Mekh. Tekhn. Fiz.* **5**, 33–38.

BORISOV, A. A., VAKHGELT, A. F. & NAKORYAKOV, V. E. 1981 Propagation of finite-amplitude perturbations in gas-particle mixtures. *Akust. Zh.* **27**, 6, 930–932.

BUEVICH, YU. A. & FEDOTOV, S. P. 1980 On weakly nonlinear perturbations in concentrated gas-particle mixtures. *Zh. Prikl. Mekh. Tekhn. Fiz.* **3**, 90–95.

CHOW, J. C. F. 1964 Attenuation of acoustic waves in dilute emulsions and suspensions. *J. Acoust. Soc. Am.* **36**, 2395–2401.

COLE, J. E. & DOBBINS, R. A. 1970 Propagation of sound through atmospheric fog. *J. Atmos. Sci.* **27**, 426–434.

COLE, J. E. & DOBBINS, R. A. 1971 Measurements of attenuation and dispersion of sound by a warm air fog. *J. Atmos. Sci.* **28**, 202–209.

DAVIDSON, G. A. 1975*a* A Burgers' equation approach to finite-amplitude acoustics in aerosol media. *J. Sound Vib.* **38**, 475–495.

DAVIDSON, G. A. 1975*b* Sound propagation in fogs. *J. Atmos. Sci.* **32**, 2201–2205.

DAVIDSON, G. A. 1976 A Burgers' equation for finite amplitude acoustics in fogs. *J. Sound Vib.* **45**, 473–485.

DAVIDSON, G. A. & SCOTT, D. S. 1973 Propagation of finite-amplitude sound through aerosols. *Proc. Symp. Finite-Amplitude Wave Eff. Fluids, Copenhagen, 1973. Guilford, 1974*, pp. 30–36.

DEICH, M. E. & FILIPPOV, G. A. 1968 *Gas Dynamics of Two-Phase Media.* Moscow: Energy.

DOBBINS, R. A. & TEMKIN, S. 1964 Measurements of particulate acoustic attenuation. *AIAA J.* **2**, 1106–1111.

EPSTEIN, P. S. & CARHART, R. R. 1953 The absorption of sound in suspensions and emulsions I. Water fog in air. *J. Acoust. Soc. Am.* **25**, 553–565.

FUKS, N. A. 1955 *Mechanics of Aerosols.* Moscow: AN SSSR Publ.

GUMEROV, N. A., IVANDAEV, A. I. & NIGMATULIN, R. I. 1983 Dispersion and dissipation of acoustic waves in gas-particulate mixtures. *Dokl. Akad. Nauk. SSSR* **272**, 560–563.

ISAKOVICH, M. A. 1948 On the propagation of sound in emulsions. *Zh. Exper. i Teor. Fiz.* **18**, 907–912.

ISAKOVICH, M. A. 1973 *General Acoustics.* Moscow: Nauka.

IVANDAEV, A. I. 1978 Propagation of weak perturbations in two-phase vapour-droplet mixtures. *Akust. Zh.* **24**, 72–78.

IVANDAEV, A. I. & NIGMATULIN, R. I. 1970 On the propagation of weak perturbations in two-phase media with phase transformations. *Zh. Prikl. Mekh. Tekhn. Fiz.* **5**, 73–77.

KLEIMAN, YA. Z. 1958 On the attenuation of harmonic waves in mixtures. *Akust. Zh.* **4**, 365–367.

KLEIMAN, YA. Z. 1961 Speed of sound in mixtures, containing suspended particles. *Akust. Zh.* **7**, 262–264.

KNUDSEN, V. O. 1931 The effect of humidity upon the absorption of sound in a room. *J. Acoust. Soc. Am.* **3**, 126–138.

KNUDSEN, V. O., WILLSON, J. V. & ANDERSON, N. S. 1948 The attenuation of sound in fog and smoke. *J. Acoust. Soc. Am.* **20**, 849–857.

LAIDLER, T. J. & RICHARDSON, E. G. 1938 The absorption of supersonics in smokes. *J. Acoust. Soc. Am.* **9**, 217–223.

LAMB, H. 1945 *Hydrodynamics.* Dover.

LANDAU, L. D. & LIFSHITZ, E. M. 1954 *Fluid Mechanics.* Moscow: *Gos. Izdat. Teor. Lit.*

LYMON, F. A. & CHEN, D. M. 1978 Acoustic attenuation in a nonuniform gas containing droplets. *AIAA J.* **16**, 503–509.

MARBLE, F. E. 1970 Dynamics of dusty gases. *Ann. Rev. Fluid Mech.* **2**, 397–446.

MARBLE, F. E. & WOOTEN, D. C. 1970 Sound attenuation in a condensing vapor. *Phys. Fluids* **13**, 2657–2664.

MEYER ZUR CAPPELEN, F. 1981 Ausbreitung von wellen kleiner amplitude in einem relaxierenden und strahlenden gas-teilchen-gemish. *Acta Mech.* **36**, 1–2; 3–39.

MORI, Y., HIJIKATA, K. & KAMADA, H. 1971 Sound velocity in gas containing small particles. *Trans. Japan Soc. Mech. Engnrs* **37**, 546–555.

NIGMATULIN, R. I. 1978 *Fundamentals of Mechanics of Heterogeneous Media.* Moscow: Nauka.

NIGMATULIN, R. I. 1979 Spatial averaging in the mechanics of heterogeneous and dispersed systems. *Intl J. Multiphase Flow* **5**, 353–385.

NIKAIEN, K., PEDDIESON, J. & AU, B. C. 1983 One-dimensional acoustic wave propagation in a particulate suspension. *Lett. Appl. Engng Sci.* **21**, 851–862.

OSWATITITSCH, KL. VON 1941 Die dispersion und absorption des shalles in wolken. *Phys. Z.* **42**, 365–378.

POPOV, V. S. 1968 On the propagation of small perturbations in gases with suspended solid particles. *Inzh.-Fiz. Zh.* **14**, 716–721.

POPOV, V. S. 1970 On sound propagation in suspensions. *Inzh.-Fiz. Zh.* **19**, 297–304.

RASMUSSEN, M. L. 1977 On wave propagation in particulate suspensions. *Trans. ASME* E: *J. Appl. Mech.* **44**, 354–355.

RICHARDSON, E. G. 1962 *Ultrasonic Physics*. Elsevier.

ROCHELLE, S. G. & PEDDIESON, J. 1976 One-dimensional wave propagation in particulate suspensions. In *Proc. 13th Soc. Engng Sci. Meeting. Rec. Adv. Engng Sci.* vol. 3, *NASA CP* 2001, pp. 947–954.

ROSENFELD, S. KH. 1983 Dispersion and absorption of sound in atmospheric fog. *Akust. Zh.* **29**, 251–256.

RYTOV, S. M., VLADIMIRSKY, V. V. & GALANIN, M. D. 1938 Sound propagation in dispersed systems. *Zh. Exper. i Teor. Fiz.* **8**, 614–621.

RYZHKOV, A. F. & TOLMACHEV, E. M. 1983 On the propagation of small perturbations in concentrated dispersed systems. *Inzh.-Fiz. Zh.* **44**, 748–755.

SEWELL, S. J. T. 1910 On the extinction of sound in a viscous atmosphere by small obstacles of cylindrical and spherical form. *Phil. Trans. R. Soc. Lond.* A **210**, 239–270.

SOO, S. L. 1960 Effect of transport processes on attenuation and dispersion in aerosols. *J. Acoust. Soc. Am.* **32**, 943–946.

SOO, S. L. 1967 *Fluid Dynamics of Multi-phase Systems*. Toronto–London: Blaisdell.

STÄDTKE, H. 1968 Speed of sound and shock waves in two phase flows. *Proc. Symp. Electr. from MHD. vol.* 3. *Warsaw. Vienna*, pp. 1313–1339.

STASENKO, A. L. 1973 On the dispersion of sound in a mixture of gas with heat-radiating macroscopic particles. *Akust. Zh.* **19**, 891–896.

TARAKANOV, S. V. & TODES, O. M. 1982 Burgers' approximation for plane long-wavelength perturbations in air-particulate mixtures. *Zh. Prikl. Mekh. i Tekhn. Fiz.* **1**, 99–106.

TEMKIN, S. & DOBBINS, R. A. 1966*a* Attenuation and dispersion of sound by particulate relaxation processes. *J. Acoust. Soc. Am.* **40**, 317–324.

TEMKIN, S. & DOBBINS, R. A. 1966*b* Measurement of attenuation and dispersion of sound by an aerosol. *J. Acoust. Soc. Am.* **40**, 1016–1024.

VIGLIN, A. 1938 Propagation of vibrations in a two-phase vapour–liquid system. *Zh. Tekhn. Fiz.* **8**, 275–285; 355–368.

WEBER, M. 1980 Schallgrenze bei Gas-Feststoff-Gemischen. *TIZ-Fachber. Rohst. Engng* **104**, 700–703.

YAMAMOTO, Y., KOBAYASHI, S. & TAKANO, A. 1980 Analysis on the propagation of finite amplitude disturbances in gas-particle mixtures. *Trans, Japan Soc. Aeronaut. Space Sci.* **22**, 229–240.

ZINK, J. W. & DELSASSO, L. P. 1958 Attenuation and dispersion of sound by solid particles suspended in air. *J. Acoust. Soc. Am.* **30**, 765–771.

ZOLOTAREV, P. P. 1964 On the propagation of weak perturbations through mixtures. *Izv. Akad. Nauk. SSSR, Mekh. i Mashinostr.* **4**, 178–180.